Bioorganic & Medicinal Chemistry Letters 20 (2010) 2391–2407

Contents lists available at ScienceDirect

Bioorganic & Medicinal Chemistry Letters

journal homepage: www.elsevier.com/locate/bmcl

Bioorganic & Medicinal Chemistry Letters Volume 20, Issue 8, 2010

Contents

ARTICLES

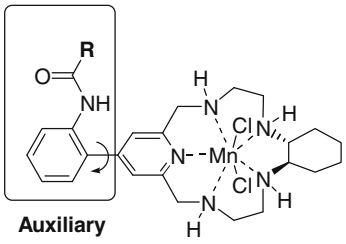

The synthesis and SOD-like activity of new manganese(II) complex of substituted pyridino pentaaza macrocyclic ligands are reported.

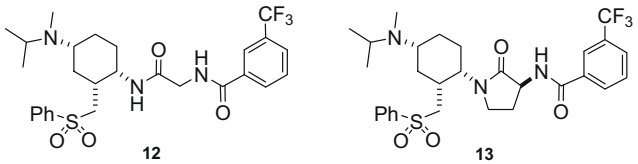

We describe the design, synthesis, and evaluation, of γ-lactams as glycinamide replacements within a series of di- and trisubstituted cyclohexane CCR2 antagonists.

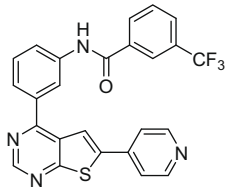

Scaffold hopping strategy was employed to replace the HTS hit scaffold pyrazolo[1,5-*a*]pyrimidine. This strategy led to the identification of additional lead compound **11b** with enhanced enzyme and cellular potency, while maintaining good selectivity over a number of kinases.

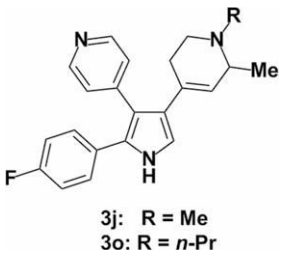

The synthesis of the proinflammatory cytokine production inhibitor **3o** (TNFα IC_{50} = 0.44 μM) and **3j** (TNFα ID_{50} = 1.42 mg/kg) are reported.

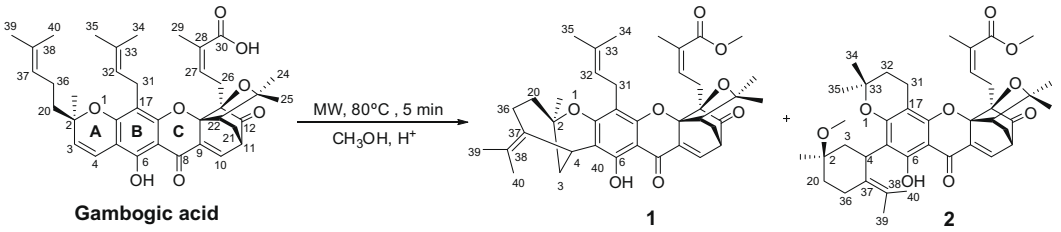

Treatment of gambogic acid with methanol in acidic condition under microwave irradiation led to the formation of two new products bearing spectacular A ring systems with promising anti-tumor effect.

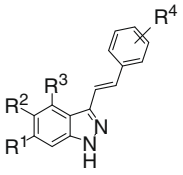

A series of alkenyl indazole derivatives were prepared and evaluated as selective Aurora inhibitors.

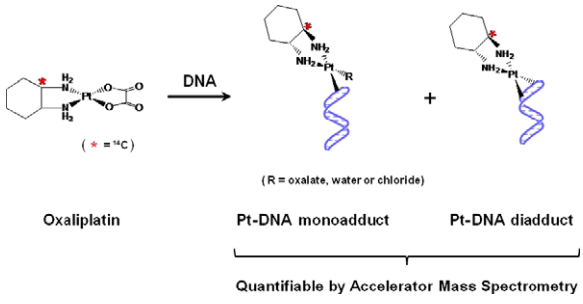

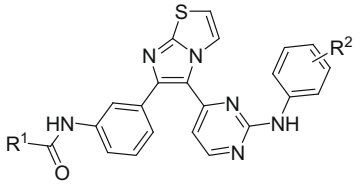

The design and enzyme activities of a novel class of imidazo[2,1-*b*]thiazoles is presented.

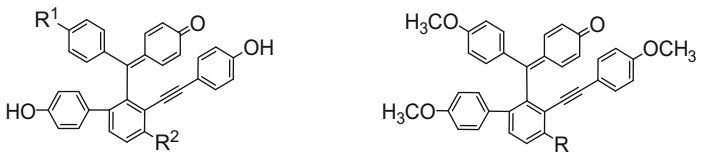

Selaginellin derivatives from *Selaginella pulvinata* with good antimicrobial activity.

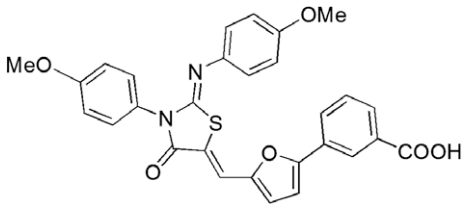

1x

The minimal inhibitory concentration (MIC), minimal bactericidal concentration (MBC) and antibiofilm concentration assay of **1x** were 6.25 μM, 25 μM and 6.25 μM against *Staphylococcus epidermidis*, respectively.

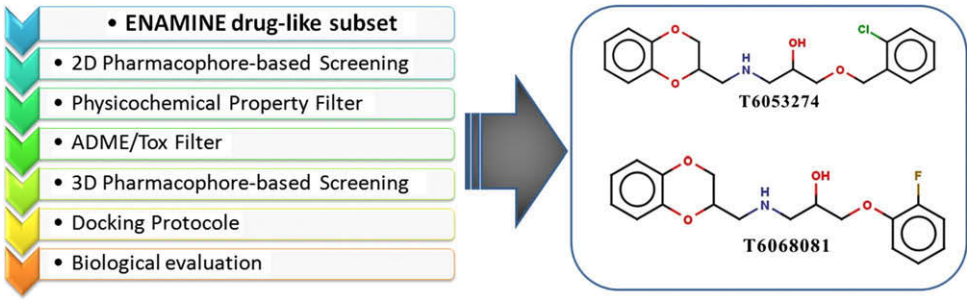

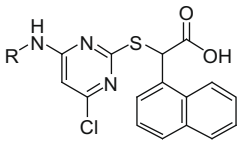

A series of pirinixic acid derivatives were synthesized and evaluated as subtype-selective peroxisome proliferator-activated receptor (PPARγ) agonists and modulator by in vitro transactivation of human PPARs.

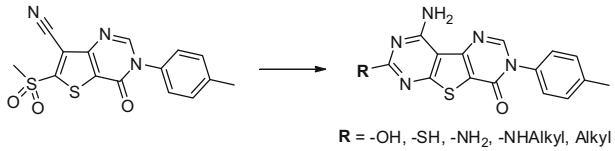

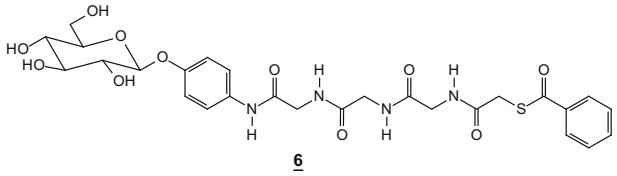

6

A D-glucose analogue was synthesized; its biodistribution studies and scintigraphic imagens were performed.

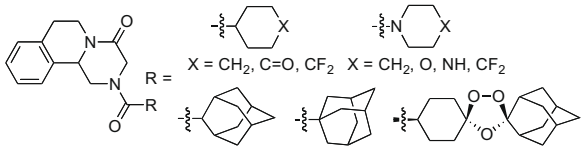

Synthesis, assaying, and computational results are reported for new anti-HIV agents that exhibit high potency and low cytotoxicity. Extension into an eastern channel in the HIV-1 reverse transcriptase binding site is investigated.

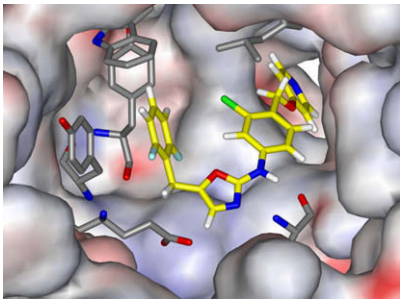

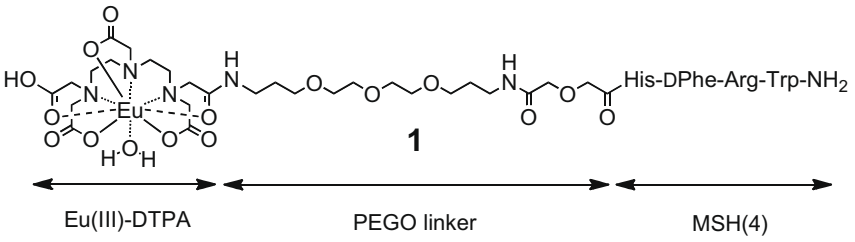

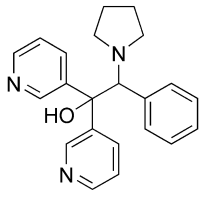

TAEA (7j)

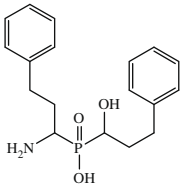

$IC_{50} = 60$ nM

New potent human aminopeptidase N (CD13) inhibitor (IC_{50} = 60 nM) is reported.

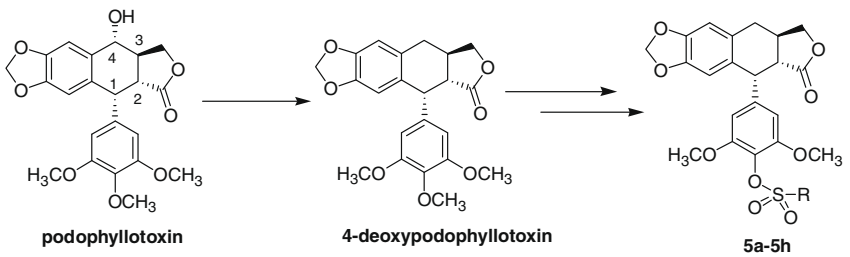

podophyllotoxin **4-deoxypodophyllotoxin** **5a-5h**

Some 4′-substituted benzenesulfonates of 4-deoxypodophyllotoxin exhibited the potent insecticidal activity.

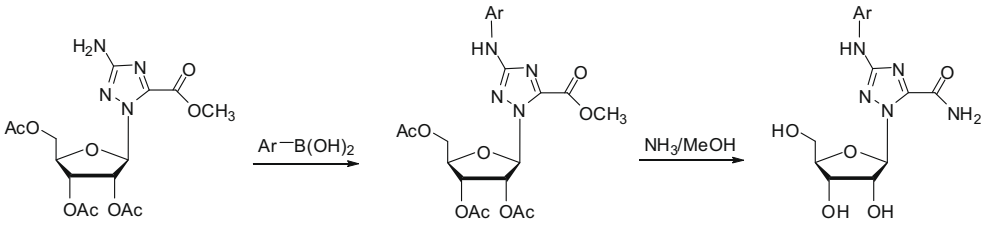

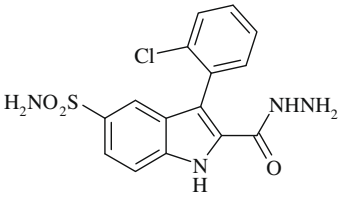

K_I = 640 nM (hCA I); K_I = 38.8 nM (hCA II); K_I = 8.0 nM (Can2); K_I = 45 nM (CaNce103).

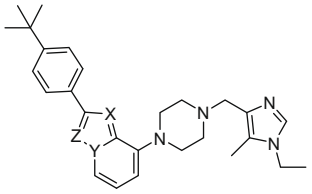

X = N(H), O, S; Y = C, N; Z = N(H), O, S

A series of bicycloheterocyclic replacements for the previously described benzimidazole template were prepared and tested for GnRH activity.

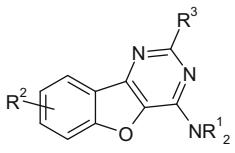

The hit-to-lead exploration of a series of novel, potent and selective series of histamine H4 receptor inverse agonists originating from a virtual screening approach is described.

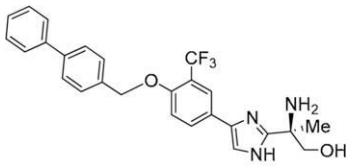

PPI-4955

Identification of a selectivity enhancing moiety has allowed for discovery of pro-drug PPI-4955 (**21b**), a potent and selective sphingosine-1-phosphate receptor-1 agonist, with excellent dose responsiveness and pharmacodynamic properties.

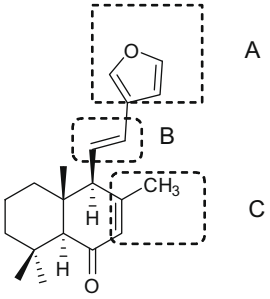

A series of analogues have been synthesized by modification of the furanoid ring, double bond and the vinylic methyl functionality of this natural product lead. All the compounds were tested for their in vitro cytotoxic activity against human cancer cell lines.

Radiosynthesis and lipophilicity of [^{11}C]Dimebon, a new potential PET agent for imaging of Alzheimer's disease and Huntington's disease, are first reported.

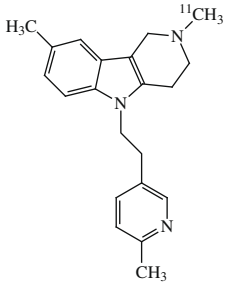

[^{11}C]Dimebon, [^{11}C]**7b**

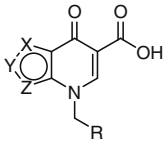

The phenyl ring in a series of quinolone carboxylic acid M_1 positive allosteric modulators was replaced with a variety of heterocycles in order to reduce protein plasma binding and enhance CNS exposure.

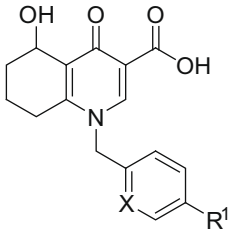

Incorporation of hydroxycycloalkyl fused pyridone carboxylic acids in lieu of quinolone carboxylic acids enhance free fraction without increased susceptibility to P-glycoprotein transport.

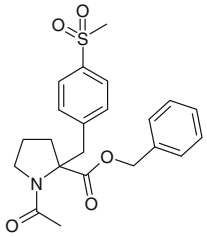

13

The benzyl prolinate **13** has been identified as a potent KCC2 blocker with selectivity versus NKCC1 and favorable ADME properties. It was evaluated in an in vivo model of epilepsy, the audiogenic mouse seizure test.

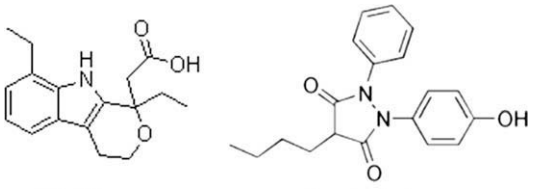

Etodolac Oxyphenbutazone

Inhibition of mouse skin cancer by non-steroidal anti-inflammatory drugs, etodolac and oxyphenbutazone is reported.

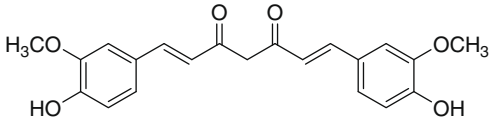

Curcumin

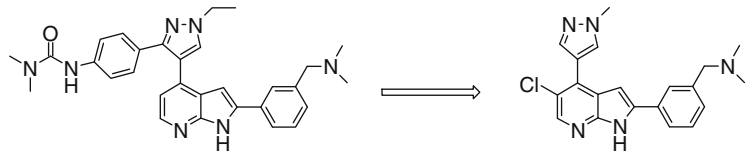

The SAR results from this investigation will be presented with an emphasis on the impact structural changes have on the cellular phenotype.

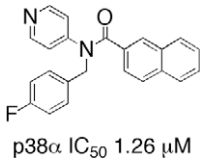

A novel series of *N*-pyridyl amide p38α kinase inhibitors is described. The proposed binding modes of the initial hits were evaluated against SAR findings to provide rationale for further development of this structural class.

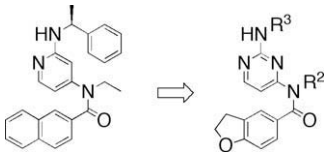

Identification and optimization of a new class of *N*-pyrimidyl amide based p38α MAP kinase inhibitors is described. The lead structure was derived from a previously reported class of pyridine-based amides. p38α activity (enzymatic/cellular) and CYP3A4 data for the new series are presented.

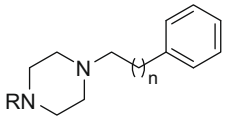

1 R = 4-pyridyl, n = 1
2 R = 4-pyridyl, n = 2
3 R = 3-pyridyl, n = 1
4 R = 3-pyridyl, n = 2
5* R = 2-pyridyl, n = 1
6* R = 2-pyridyl, n = 2

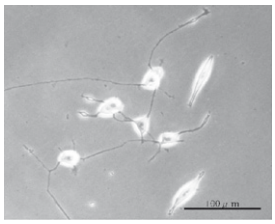

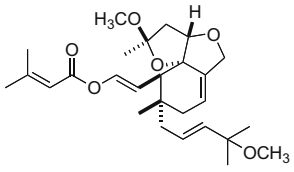

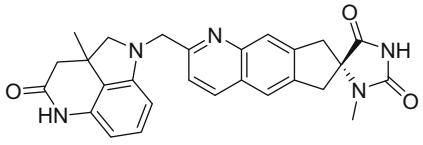

19 K_i = 0.52 nM

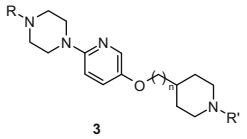

3

A series of 2-piperazinyl-5-alkoxypyridines (**3**) were synthesized and screened against human GPR119 receptor. Through SAR analysis, compounds containing 2-alkylsulfonylpiperazinyl-5-alkoxypyridines were discovered and found to be potent agonists of the human GPR119 receptor.

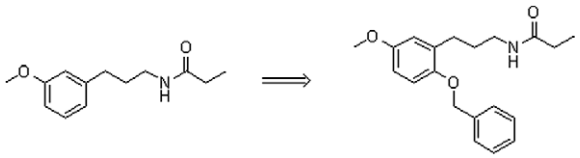

1b **2b**

MT_2 Ki = 7.07 nM MT_2 Ki = 0.55 pM

A benzyloxyl substituent incorporated at C6 position of the 3-methoxyphenyl ring dramatically enhanced the melatonin MT_2-binding affinity.

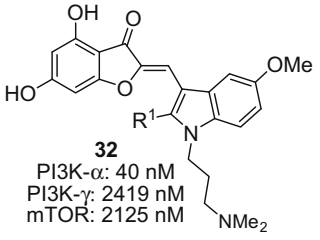

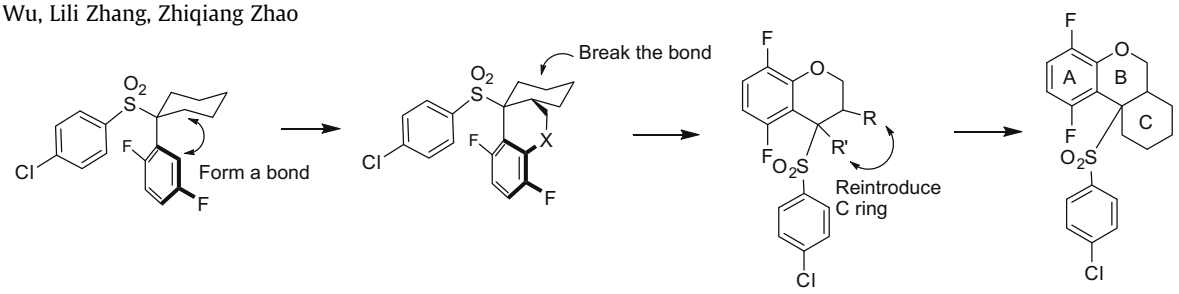

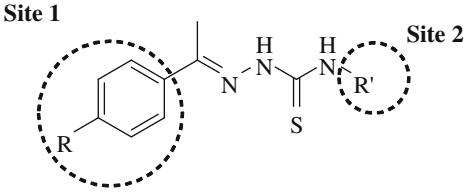

A series of novel substituted hydrazinecarbothioamides was synthesized and evaluated for anti-TB activity. Three most active compounds viz. **1**, **6** and **12** were found to exhibit minimum inhibitory concentration (MIC) of 0.4 μg/mL whereas four compounds viz. **3**, **5**, **10** and **11** showed comparatively lesser activity with MIC value of 0.8 μg/mL against *Mycobacterium tuberculosis* strain. A highly significant QSAR equation explaining 81.8% variance is described.

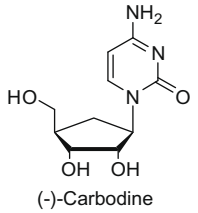

Enantiomerically pure cyclopentyl cytosine [(−)-carbodine] exhibited potent antiviral activity against H5N1 (avian) and novel H1N1 (swine) flu.

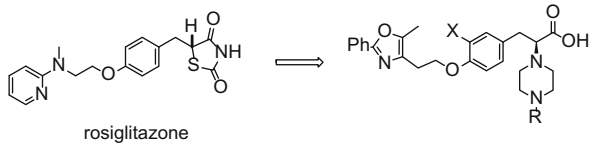

A series of novel, potent PPARα/γ dual agonists were synthesized and appraised. Compound **2b** was chosen for further in vivo evaluation in the *db*/*db* mice, rosiglitazone were used for comparison.

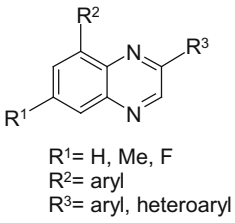

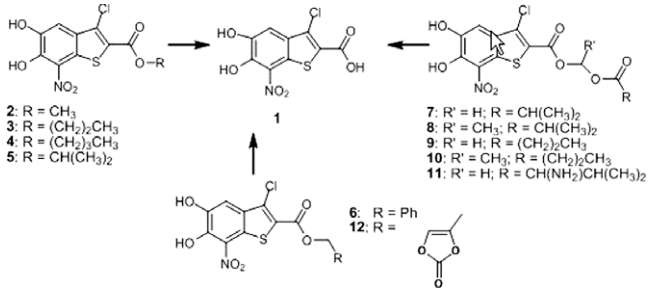

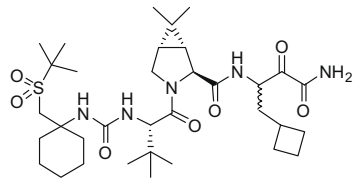

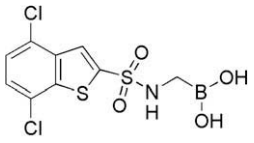

DSABA

4,7-Dichloro-1-benzothien-2-yl sulfonylaminomethyl boronic acid (DSABA) is reported as the first boronic acid-based class D beta-lactamase inhibitor, also with class A and C activity.

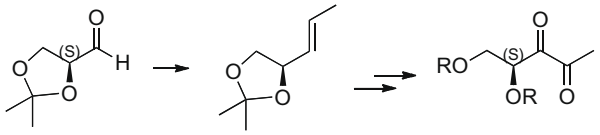

Synthesis of both enantiomers of autoinducer DPD (shown (*S*), R = H) along with their ester bioprecursors (R = Bz, Ac) & biological assays.

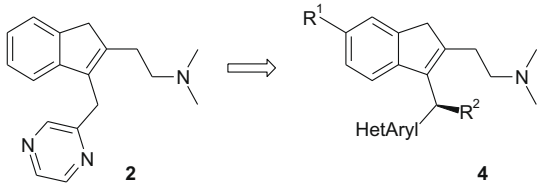

2 **4**

Structure–activity relationships were conducted around a lead H_1-antihistamine **2**, to identify selective analogs with the potential for reduced biotransformation through the CYP2D6 pathway. A number of candidate compounds were identified from the general structure **4** using the appropriate combination of electron rich heterocycles, the presence of a chiral center and 6-substitution in the indene core.

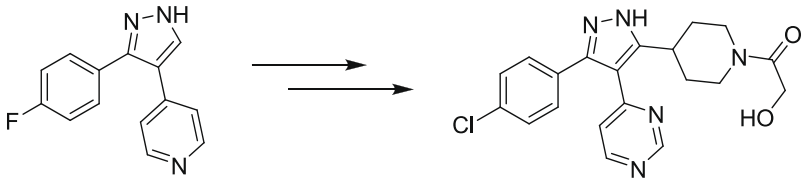

SC-102 SD-0006

Starting from the novel screening lead, SC-102, synthesis and structure activity relationships are provided highlighting the progression to and identification of the potent p38 MAP kinase inhibitor SD-0006.

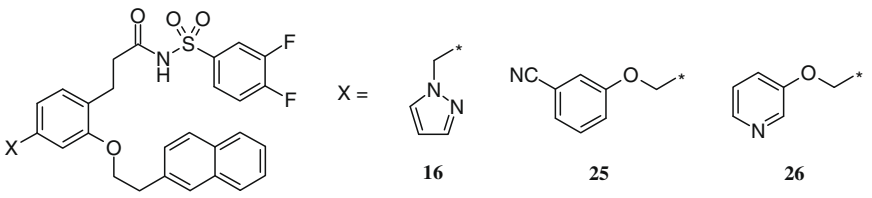

Identification of novel *N*-acyl 3,4-difluorobenzenesulfonamide analogs as potent and selective EP3 receptor antagonists and their in vivo efficacy with respect to the PGE_2-induced uterine contraction in pregnant rats are reported.

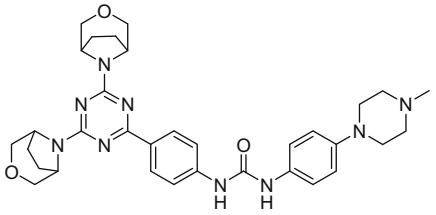

Incorporation of bridged morpholines in monocyclic triazine PI3K/mTOR inhibitors gave compounds with increased mTOR selectivity relative to the corresponding morpholine analogs leading to compounds which suppressed mTOR biomarkers in vivo and possessed excellent efficacy in a murine xenograft model.

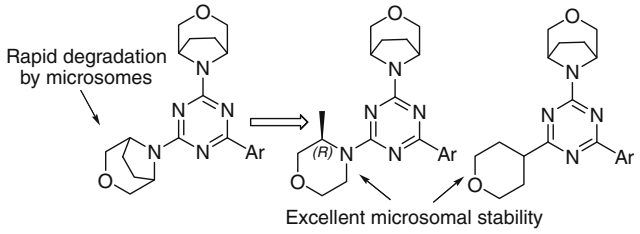

Isosteric replacement of one of the 3,5-ethylene-bridged morpholines in triazine mTOR inhibitors led to significant improvements in human microsomal stability, resulting in a compound that selectively suppressed mTOR biomarkers in vivo and possessed excellent efficacy in a murine xenograft model.

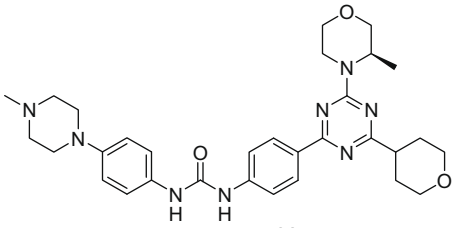

Potent inhibitors of the mammalian target of rapamycin (mTOR) which contain the triazine scaffold and the (*R*)-3-methyl morpholine moiety have been identified. Such compounds also displayed excellent cellular activity and good selectivity over the related lipid kinase PI3Kα.

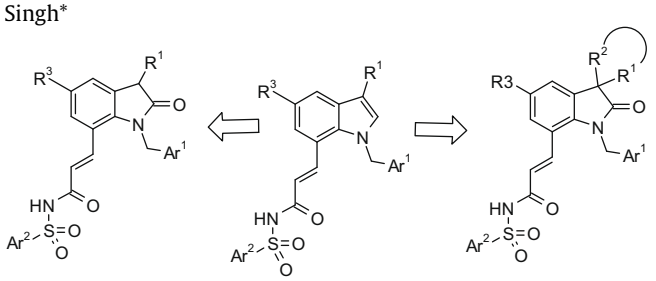

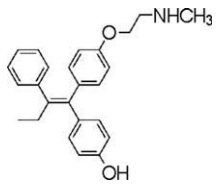

A novel synthesis of endoxifen and its PKC inhibitory activity is reported.

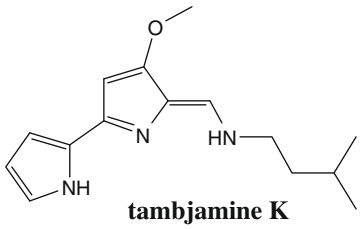

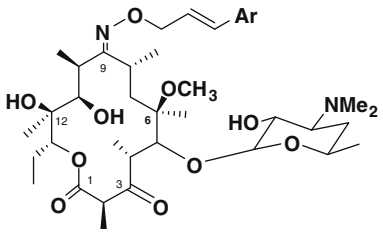

New 9-*O*-arylpropenyloxime ketolides were synthesized and evaluated their antibacterial activities against clinically isolated gram-positive strains. The SAR is discussed.

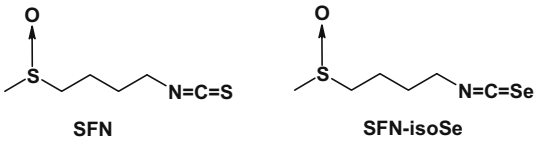

SFN-isoSe, an isosteric selenium analog of naturally occurring sulforaphane (SFN), is a potent inducer of the Nrf2/ARE pathway and may represent a more effective chemoprotective agent in vivo.

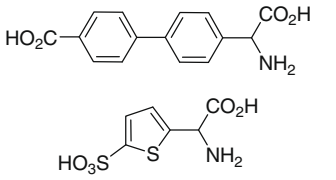

block approx. 75% uptake of system x_c^-

*Corresponding author
ⓘ+ Supplementary data available via ScienceDirect

COVER

Overlay of high resolution co-crystal structures of *R*-**22**-ADP (cyan) and **1**-ADP (green) bound in an allosteric binding site of the mitotic kinesin KSP. [Roecker, A. J.; Coleman, P. J.; Mercer, S. P.; Schreier, J. D.; Buser, C. A.; Walsh, E. S.; Hamilton, K.; Lobell, R. B.; Tao, W.; Diehl, R. E.; South, V. J.; Davide, J. P.; Kohl, N. E.; Yan, Y.; Kuo, L. C.; Li, C.; Fernandez-Metzler, C.; Mahan, E. A.; Prueksaritanont, T.; Hartman, G. D. *Bioorg. Med. Chem. Lett.* **2007**, *17*, 5677.]

Indexed/Abstracted in: Beilstein, Biochemistry & Biophysics Citation Index, CANCERLIT, Chemical Abstracts, Chemistry Citation Index, Current Awareness in Biological Sciences/BIOBASE, Current Contents: Life Sciences, EMBASE/Excerpta Medica, MEDLINE, PASCAL, Research Alert, Science Citation Index, SciSearch, TOXFILE. Also covered in the abstract and citation database SCOPUS®. Full text available on ScienceDirect®

ELSEVIER

ISSN 0960-894X